

Rising Air-Conditioning Use Intensifies Global Warming

Received: 26 July 2024

Accepted: 27 January 2026

Published online: 25 February 2026

 Check for updates

Hongzhi Zhang ^{1,2,3,4}, Yuli Shan  ³, Ruoqi Li^{3,5,14}, Rui Xue⁶, Junhua Ma⁷, Jarmo Kikstra ^{8,9,10}, Zongbo Shi ³, Zhaohua Wang ^{1,2,4} , Bin Zhang ^{2,4,11}, Bo Wang ^{2,4,11}, Shuai Fang¹², Fan Yang ¹³ & Klaus Hubacek ¹⁴

Global warming and socio-economic development are together prompting a surge in the use of air-conditioning (AC). Yet the technology that delivers thermal comfort also emits large quantities of greenhouse gases (GHG), exacerbating climate change. We quantify global AC-related GHGs and associated warming impact under five climate scenarios, separating the contributions of global warming and socio-economic development. In a middle-of-the-road scenario (SSP245), cumulative AC-related emissions reach 113.3 GtCO₂eq between 2010 and 2050, increasing global-mean temperature by 0.05 °C (0.03 °C–0.07 °C), with only about 8.3% to climate-driven cooling demand. Income inequalities exacerbate disparities in AC use, substantially limiting access to cooling in lower-income regions. While rising incomes reduce this inequality, they increase emissions: income-driven AC growth adds 14–146 GtCO₂eq and a further 0.003–0.05 °C of warming by 2050, even under SSP119. These results highlight the need for a rapid low-carbon cooling transition that balances total warming impacts with equitable cooling access.

Excessive anthropogenic GHG emissions have already warmed the planet by 1.2 ± 0.1 °C since the pre-industrial era¹. The resulting rise in surface temperatures, together with more frequent and intense heat-waves, has caused nearly half a million heat-related excess deaths between 2000 and 2019^{2,3}. Air-conditioning is an effective and widely used adaptation measure for protecting people from hazardous heat⁴. In parallel, rapid economic expansion in emerging economies, growing urban populations, and falling prices of appliances have expanded access to AC-based space cooling, transforming latent thermal-comfort demand into an unprecedented surge in AC adoption⁴.

Consequently, the joint influence of global warming and socio-economic development produced a four-fold surge in annual global air-conditioner sales from 1990 to 2016^{4,5}, with over half located in China and the United States⁶.

Although the widespread AC use facilitates human adaptation to hot and humid weather, it also brings about additional energy consumption and resulting GHG emissions^{5,7}. Given that cooling largely relies on electricity, this strategy has led to a more than threefold increase in global electricity consumption for cooling from 1990 to 2016⁴. Some regions (e.g., the United States and the Middle East) even

¹School of Economics, Beijing Institute of Technology, Beijing, China. ²Center for Sustainable Development and Smart Decision, Beijing Institute of Technology, Beijing, China. ³School of Geography, Earth and Environmental Sciences, University of Birmingham, Birmingham, UK. ⁴Digital Economy and Policy Intelligentization Key Laboratory of Ministry of Industry and Information Technology, Beijing, China. ⁵State Key Laboratory of Water Pollution Control and Green Resource Recycling, School of the Environment, Nanjing University, Nanjing, China. ⁶La Trobe Business School, La Trobe University, Melbourne, VIC, Australia. ⁷Faculty of Management and Economics, Kunming University of Science and Technology, Kunming, China. ⁸International Institute for Applied Systems Analysis (IIASA), Laxenburg, Austria. ⁹Grantham Institute for Climate Change and the Environment, Imperial College London, London, UK. ¹⁰Centre for Environmental Policy, Imperial College London, London, UK. ¹¹School of Management, Beijing Institute of Technology, Beijing, China. ¹²Business School, Soochow University, Donghuan Road 50, Suzhou, China. ¹³Department of Planning, Aalborg University, Aalborg, Denmark. ¹⁴Integrated Research on Energy, Environment and Society (IREES), Energy and Sustainability Research Institute Groningen, University of Groningen, Groningen, the Netherlands.

 e-mail: y.shan@bham.ac.uk; wangzhaohua@bit.edu.cn

have an AC demand accounting for over 50% of their peak electricity load on hot days⁸. Considering that our current power generation is mainly based on fossil fuels^{9,10}, the increase in electricity use for air-conditioning could cause substantial GHG emissions in the near-term. Refrigerants used in air conditioners, such as hydrofluorocarbons (HFCs), chlorofluorocarbons (CFCs) and hydrochlorofluorocarbons (HCFCs), also contribute considerably to global warming if leaked to the air¹¹. Consequently, expanding AC access presents a fundamental trade-off: it safeguards human well-being in hotter climates while simultaneously locking in additional warming impact through both energy and refrigerant pathways. Quantifying and mitigating this climate penalty is therefore essential to ensure that gains in thermal comfort do not undermine long-term mitigation goals.

There have been emerging discussions around the trade-offs between the thermal benefits of increasing AC use and its associated GHG footprints^{12,13}. Yet no study has quantified how the interactions between socio-economic development and global warming across climate scenarios could shape future AC demand, nor how that demand, in turn, could feed back to global-mean temperature. Existing analyses have not investigated the respective contributions of socio-economic drivers (such as income growth and population) and climatic drivers to future AC uptake and total warming impact. More importantly, although current income-driven inequalities in AC use are well documented, there are only few studies focusing on systematic quantification of future cooling inequalities. The additional emissions and associated warming impact that would accompany low-income households attaining higher living standards are still unaccounted for¹⁴. In addition, existing research often fails to account for the influence of relative humidity (RH) on cooling demand and neglected regional variations in AC demand¹⁵. Finally, only a few studies have examined the cooling sector under high-emission scenarios (e.g. RCP8.5) at the regional and global scales within an integrated framework, utilizing detailed energy-system models and General Circulation models (GCMs)^{7,16,17}. However, these studies overlooked the large uncertainties arising from limited GCM ensembles, and crucially, they have not explored the long-term impacts of low-carbon transition driven by stringent climate targets on the warming impact caused by AC use.

Aiming at the above research gap, our study seeks to quantify the total warming impact from AC use on global-mean temperature across scenarios, investigate the respective contributions of socio-economic development and global warming, and evaluate how narrowing income-driven cooling inequalities reshapes both emissions and warming potential. Therefore, we design an integrated approach that incorporates the improved cooling degree days (CDD) approach, the Global Change Analysis Model^{18,19} (GCAM), and the Model for the Assessment of Greenhouse Gas Induced Climate Change (MAGICC, <https://magicc.org/>)^{20–22}. Our projection of future regional CDDs is enhanced by introducing the heat-index approach and multi-model simulation from 25 widely applied GCMs (see Supplementary Table 1), providing a more comprehensive and nuanced estimation of cooling demand across regions (see “Methods”). GCAM provides a series of detailed functions for cooling services and energy demands, leveraging the dynamic interactions between socio-economic development, complex energy systems and climate change to capture cooling energy demand at both global and regional scales. By incorporating projected CDDs across scenarios, we employ GCAM to estimate AC energy consumption for cooling and the associated GHG emissions under the five SSP-RCP scenarios (see “Methods”). We also quantify the respective contributing effects of socio-economic factors (e.g., floor-space, GDP, income, and population) and global warming (e.g., CDDs) to the trajectories of AC stock and energy consumption. Moreover, we use the well-calibrated climate emulator MAGICC v7.5.3 to quantify the possible ranges of additional warming effects from AC use (see “Methods”). To investigate the climate-driven feedback and socio-

economic contributions of AC-induced global warming impacts, we construct simplified counterfactual experiments within our IAM framework across scenarios. Finally, we assess the inequality in cooling services using Lorenz curves and Gini coefficients based on cooling energy consumption and expenditure derived from the GCAM, and develop an econometric model to quantify these inequalities in the cooling gaps (the unmet need for air-conditioning due to a lack of income) through AC stock under different income levels within SSP-RCP scenarios (see Methods). Our study provides quantitative global insights on the impact of AC use with the interactions between the changing climate and socio-economic development, exploring the extent of warming impact and cooling vulnerabilities.

We employ two widely used scenario frameworks to build future climate simulations: the Representative Concentration Pathways (RCPs) and Shared Socioeconomic Pathways (SSPs). Following the scenarios highlighted by Working Group I of the IPCC Sixth Assessment Report (AR6)^{23,24}, we use the SSP119 (referred as SSP1-RCPI.9), SSP126, SSP245, SSP370 and SSP585 scenarios as a range of future climate mitigation scenarios, matching with the climate projections in CMIP6 (Coupled Model Intercomparison Project Phase 6)^{25,26} and NASA NEX-GDDP-CMIP6 dataset. SSP126, SSP245, and SSP585 represent, respectively, a world on a sustainable pathway, medium development, and high dependence on fossil energy^{27,28}. SSP119 and SSP370 emphasize scenarios, respectively, with lower emissions to achieve the 1.5 °C target and significant developmental disparities between regions (see “Methods”)^{29,30}.

Results

Impacts of global warming on cooling demand

Figure 1 shows global cooling demand trends under the five SSP-RCP scenarios. We account for the cooling demand consistent with the GCAM regional classification (see Supplementary Table 2). We use population-weighted Cooling Degree Days (CDDs) to measure historical and future cooling demand both globally and within regions using mean surface temperature and relative humidity gridded data (0.25°x 0.25°, -25 km), and global 1 km downscaled population distribution gridded data. Gridded data of temperature and relative humidity come from the CMIP6 database²⁶ and the NASA NEX-GDDP-CMIP6 dataset, and population distribution from the NASA Socioeconomic Data and Applications Center (SEDAC database)^{31,32}.

Global cooling demand, measured in CDDs, is projected to increase by an average of 25% across climate models (–5% to 100%, ranging across 25 GCMs) by 2050 under the baseline scenario (SSP245) compared to 2010 (see Fig. 1a). By 2100, this increase is expected to reach 50% with a range of 12% to 160%. Due to the most stringent GHG emission control, global CDDs under the SSP119 scenario (Fig. 1c) show a slight increase, with a 4% rise in 2100 relative to 2010, remaining far below the other scenarios. Despite a 28% increase in global cooling demand from 2010 to 2050 under the SSP126 scenario, the widespread adoption of negative carbon technologies, similar to those in the SSP119 scenario, results in a lower global CDD in 2100 compared to 2050. By contrast, under high-emission scenarios (SSP370 and SSP585), global cooling demand is projected to increase considerably, particularly as GHG emissions accumulate, with demand in 2100 being substantially higher than in 2050 (with 48% and 66%, respectively).

From a regional perspective, higher-emission scenarios generally result in considerably higher cooling demand across all regions by the end of the century, while lower-emission scenarios lead to lower cooling demand. In contrast, by 2050, the expected rise in cooling demand under higher-emission scenarios does not emerge uniformly across all regions, suggesting an uneven distribution across regions in the mid-term projections. Several interconnected factors explain such discrepancies. First, regions responding most rapidly to climate change are primarily located in the high latitudes of the Northern Hemisphere, but they contribute relatively little to global CDDs²¹. For

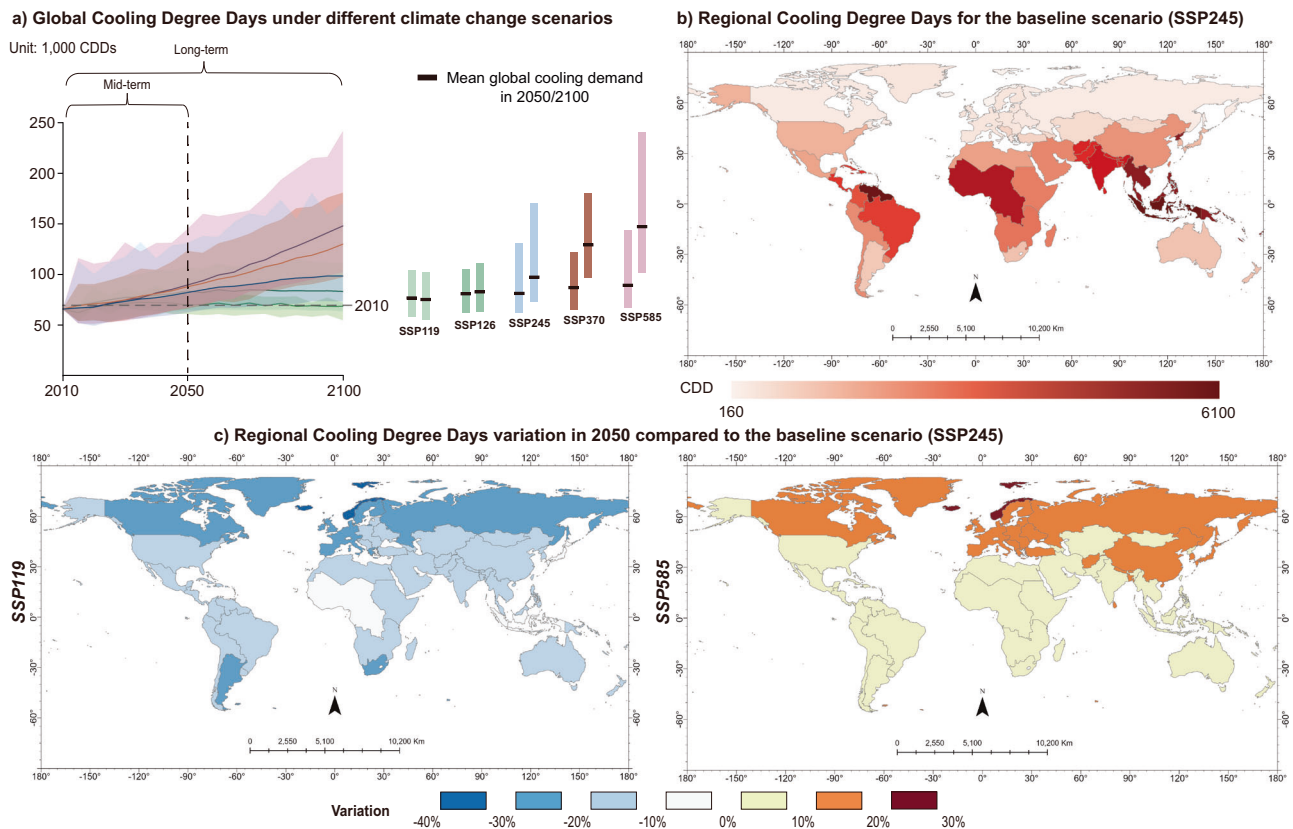


Fig. 1 | Global cooling demand trends under different climate change scenarios.

a Global Cooling Degree Days under different SSP-RCP scenarios. Global CDDs represent the total population-weighted CDDs (unit: 1000 CDDs) during the time period 2010–2100. The color lines represent mean population-weighted CDDs during 2015–2100 across five SSP-RCP scenarios. The shadows and bars represent wide ranges of global population-weighted CDDs in 2050/2100 from 25 GCM

outputs; **b** Detailed regional CDDs in 2050 under the baseline scenario (SSP245). **c** Regional cooling demand variation by 2050 under other scenarios compared to the baseline. Red and blue represent increased and reduced regional CDDs compared to the baseline scenario, respectively. Regional CDD variation under the SSP126 and SSP585 scenarios is shown in Supplementary Fig. 1.

example, under the SSP119 scenario, cooling demand in Northern Hemisphere regions, such as Canada and Northern Europe, declines considerably by 2050; however, it does not fully offset the increases in other regions, contributing to a slight increase in global CDDs from 2010 to 2050. Second, ambitious mitigation policies in low-emission scenarios (SSP119 and SSP126) reduce aerosol concentrations²⁹, which have previously exerted a short-lived cooling effect^{33,34}. Consequently, diminishing aerosol-related cooling can lead to temperature rise and greater cooling demand in regions such as West Africa and South Asia³⁵. Furthermore, demographic shifts can also affect regional cooling demand in the mid-term. For instance, under the SSP126 scenario, a relative increase in populations residing in warmer regions (e.g., Australia and New Zealand) contributes to higher cooling demand than under the baseline scenario. Conversely, projected population decline in regions such as Canada and Russia under the SSP370 scenario leads to reduced cooling demand compared to the baseline scenario. Taken together, these results highlight the intricate interplay between climate dynamics, aerosol forcing, and demographic changes that shape heterogeneous regional cooling demand in the mid-term.

Moreover, there is a considerable mismatch between regional cooling demand and economic development. The distribution of current and future cooling demand differs considerably across regions³⁶: most of the cooling demand is concentrated in equatorial regions. Figure 1b shows that Southeast Asia have the highest CDDs of 6105 in 2050 under the baseline scenario, followed by Indonesia (6091) and the northern part of South America (5409). However, regions with substantial cooling demand (over 4000 CDDs), such as Pakistan, Western Africa, and South Asia, are often those with the lowest

economic development³⁷. Conversely, many high-income regions, such as Canada and European regions, typically exhibit cooling demand below 1000 CDDs. This economic divide is further highlighted by the fact that the five low-income regions, whose combined GDPs amounts to merely 14% of that of the five high-income regions, nevertheless account for 24.4% of global cooling demand, whereas these high-income regions contribute just 8.7%.

Air-conditioning stock and energy consumption

The extent to which global cooling demand could affect the AC stock is dependent on economic development^{9,38}. Under the middle-of-the-road baseline scenario (SSP245), global AC stock is projected to be around 2.3 (1.9–3.4) billion units in 2050 (see Fig. 2a). The highest increases are found in the scenario that combines strong economic growth with high levels of global warming (SSP585), reaching 3.1 billion units in 2050. The sustainable development and “well below 2°C” mitigation scenario (SSP126) also shows higher AC demand than the baseline, at 2.6 billion units. Due to slow economic development, the SSP370 scenario has the lowest AC stock (2.0 billion), even 14% lower than that under the SSP119 scenario.

Similarly to AC stock trends, global AC energy consumption is largely determined by economic development and cooling demand. Under the baseline scenario, global AC energy consumption is projected to increase by 135.7% in 2050 compared to 2010 (See Fig. 2b). Despite the variety of AC types, the use of air-conditioning is mostly powered by electricity³⁹, with a very small portion provided by natural gas. AC electricity consumption contributes 8.0% of total energy consumption (TEC) globally in the building sector in 2050, reaching

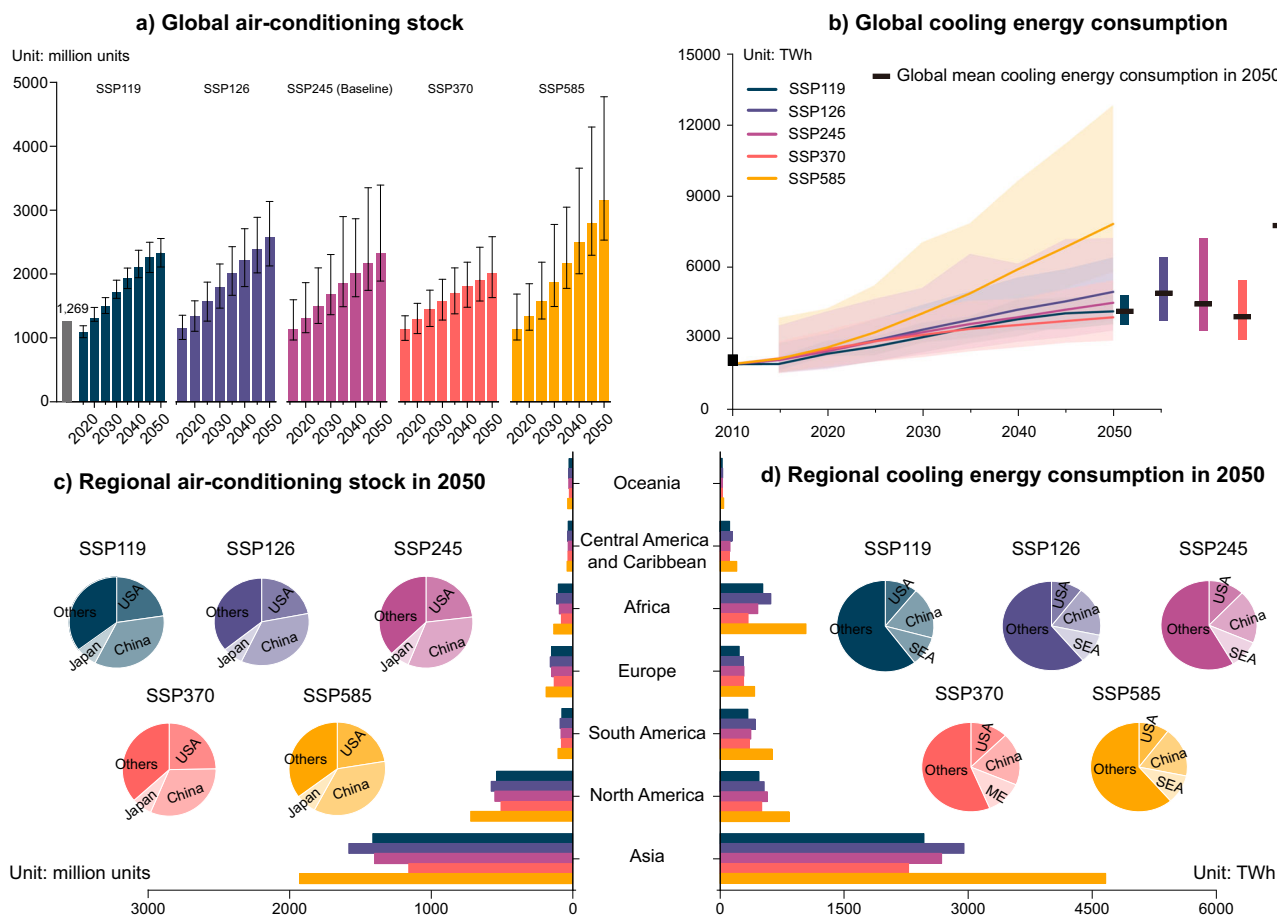


Fig. 2 | Global and regional AC stock and cooling energy consumption.

a, b Global AC stock (Unit: in million AC units) and cooling energy consumption (Unit: TWh) across five SSP-RCP scenarios. **c, d** Regional AC stock and cooling energy consumption in 2050. The bars and lines represent AC stock and cooling demand estimated based on global mean CDDs. The error bars and shadows

represent possible ranges of global AC stock and cooling energy consumption based on the range of global cooling demand under five climate scenarios. The gray bar and square represent historical data from IEA⁴ and GCAM, respectively. ME and SEA respectively represent the Middle East and Southeast Asia.

4493 (3326–7225) TWh, aligning similarly with previous studies that estimate around 4000 TWh by 2050⁴⁰. Driven by high cooling demand and per capita GDP, the SSP585 scenario consumes the most AC-related electricity among all scenarios, ranging from around 5800 to 12,821 TWh, which accounts for up to 14.9% of TEC in the building sector globally. Even though the cooling demand in the SSP126 scenario is lower compared to the SSP370 scenario, higher per capita income still results in more AC electricity consumption by 2050, which aligns with previous studies indicating that income drives a large increase in cooling energy consumption under the SSP1 pathway⁴¹. Although the SSP370 scenario projects the lowest overall AC energy consumption, the reduction compared to the SSP119 scenario (~6%) is relatively smaller than the corresponding difference in AC stock. This diminished gap, beyond potential methodological mismatches between the stock and consumption modeling approaches (as discussed in Limitations), can be attributed to the interplay between various factors, including differences in cooling demand, usage patterns, and energy efficiency. For example, compared to the SSP119 scenario, the higher cooling demand projected under the SSP370 scenario leads to longer AC operating hours or more intensive usage (Unit energy consumption) (see Supplementary Fig. 2). Furthermore, the narrative of the SSP370 scenario assumes slower technological progress, implying lower building energy efficiency relative to the SSP119 scenario. The combination of potentially higher usage intensity and lower unit efficiency in SSP370 substantially offsets the reduction in aggregate energy

consumption that would otherwise be expected from its considerably smaller AC stock.

Income growth has been found as the dominant driver of the potential surge in both installed AC stock and associated energy consumption. Our decomposition analysis shows that, averaged across the five SSP-RCP scenarios, the income effect alone contributes to 158% of the increase in the global AC stock and 190% of the increase in global AC energy consumption between 2010 and 2050 (see Supplementary Table 3 to 4). For the global AC stock, the next two largest growth drivers are the AC penetration intensity effect (captures changes in the number of installed AC units relative to the cooling demand) and population effect, which raise the stock by 74% and 40%, respectively. By contrast, the floorspace intensity effect produces the greatest decreasing effect, because aggregate economic output has expanded more rapidly than total floor area. These drivers exert similar effects on global AC energy consumption.

Because those income gains are unevenly distributed, their imprint on cooling demand is highly diversified regionally. Across all scenarios, AC stock and energy consumption of China and the United States far outweigh stock and consumption in other regions. With the additional contributions from Japan, the Middle East and Southeast Asia, Asia is projected to emerge as the leader in this aspect (see Fig. 2c, d). The decomposition analysis confirms these contrasts: the income effect results in 318.2% of the increase in AC stock and 395.5% of the increase in cooling energy consumption in China, whereas in the United States, it leads to only 73.2% and 64.2% increases,

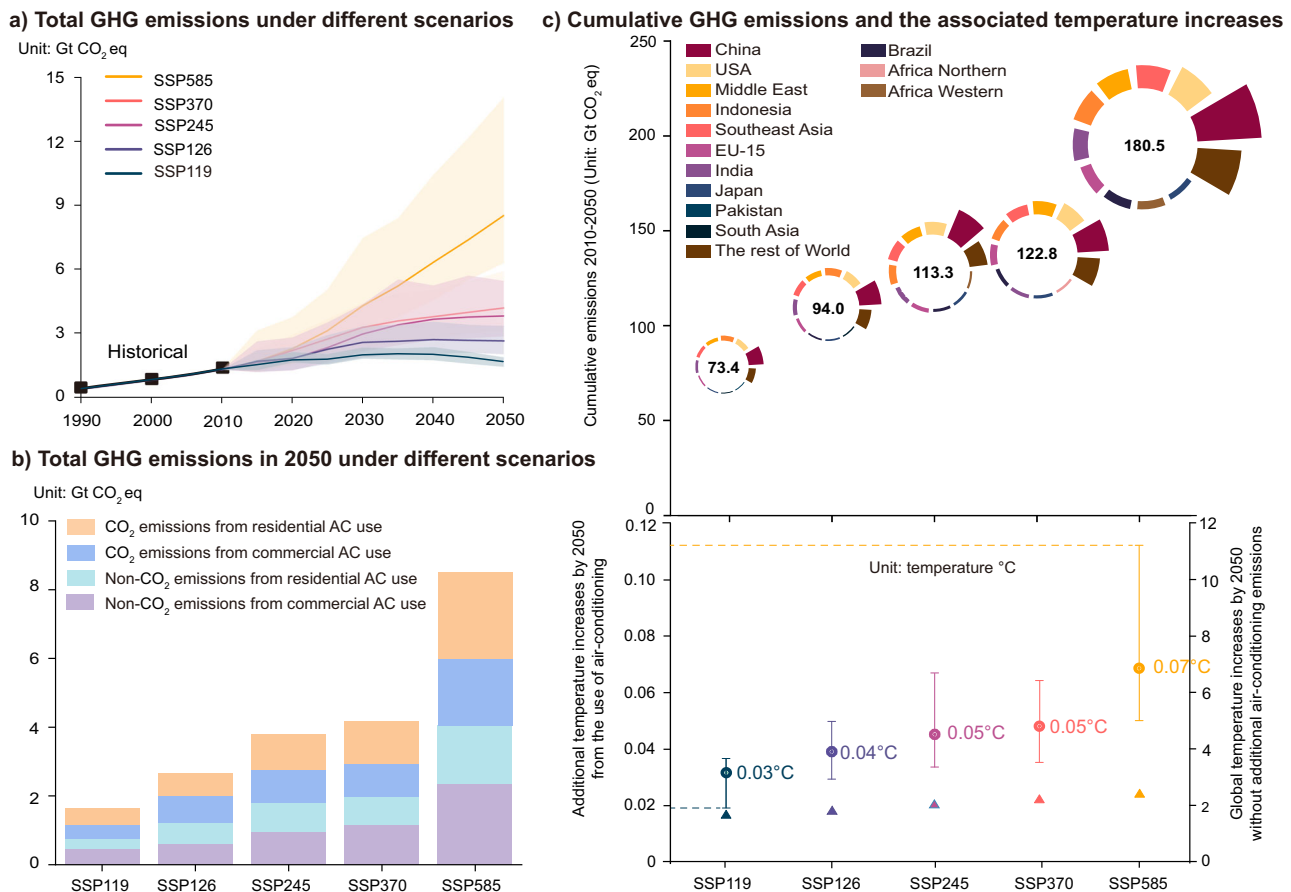


Fig. 3 | GHG emissions and the resulting warming effects produced from AC use. **a** Total GHG emissions across five SSP-RCP scenarios. The lines represent the GHG emissions based on mean CDD, while the shadows represent possible ranges of GHG emissions based on min and max CDD. **b** Total GHG emissions in 2050 by fuel and emitter. Total GHG emissions associated with AC use are categorized into four emission sources across two building types: residential and commercial. In residential buildings, CO₂ emissions from AC use comprise -0.6% from natural gas consumption by gas-powered ACs and 99.4% from electricity consumption. In commercial buildings, CO₂ emissions account for about 0.5% from natural gas consumption and 99.5% from electricity consumption. Non-CO₂ emissions from AC use are from two sources: refrigerant leaks from AC use and other non-CO₂ emissions from power transmission. Regarding the types of AC refrigerants, the default settings of GCAM account for traditional refrigerants,

such as HFC-134a and HFC-143a, as well as the low-GWP refrigerant HFC-32. Non-CO₂ emissions from residential and commercial AC use are primarily derived from AC refrigerants (-98.9%), with a minor contribution from power transmission (approximately 1.1%). **c** Global cumulative GHG emissions and the associated warming effects across scenarios. Triangles in the figure represent the reference warming temperatures for each SSP-RCP scenario, with the dots indicating the additional warming effects caused by the average GHG emissions resulting from AC use. Owing to rounding, the warming contributions for SSP245 and SSP370 appear similar; in fact, the SSP370 value (0.048 °C) is slightly higher than that for the SSP245 scenario (0.045 °C). The error bars denote the range of temperature increases based on the range of global cooling demand under five climate scenarios.

respectively. Similar disparities emerge elsewhere. In rapidly urbanizing economies such as Africa, India and Indonesia, lagging efficiency and steep income growth together drive the fastest proportional increases in both metrics. Although per capita levels in these regions remain below those in China due to income constraints, ongoing urban population growth and rising incomes suggest that future AC uptake and cooling energy consumption in these regions could exceed our current projections⁴².

Contribution of air-conditioning use to global warming

GHG emissions from AC use are projected to peak before 2040 under the ambitious climate mitigation scenarios (SSP119 and SSP126) but continue to increase until 2050 in other scenarios (see Fig. 3a). The emissions from AC use are largely determined by how clean the power generation supply is (see Supplementary Fig. 3), given that electricity is the main energy source. Under the baseline scenario, AC-related GHG emissions increase from 1.3 GtCO₂eq in 2010 to 3.8 (2.9–5.5) GtCO₂eq in 2050. The SSP585 scenario generates the largest GHG emissions. Considering the highest share of fossil fuel involved with power supply

in all scenarios, GHG emissions from AC use under the SSP585 scenario reach about 8.5 (6.2–14.0) GtCO₂eq in 2050, approximately equivalent to the total CO₂ emissions of the United States in the last two years⁴³. The SSP370 scenario consumes less energy for air-conditioning relative to the baseline scenario, but still produces more GHG emissions, reaching 4.2 (3.1–5.9) GtCO₂eq in 2050. The underlying reason is similar: the assumed share of fossil fuels in the power supply under the SSP370 scenario (72.7%) is larger than under the baseline scenario (66.6%, including the share of CCS technology). However, when low-carbon energy dominates the power supply structure, the situation would be very different. For example, under the SSP126 scenario, GHG emissions from AC use decline by 30.5% (11.9%–46.6%) in 2050 relative to baseline, even with 10.2% higher energy consumption for air-conditioning. In contrast to the SSP585 scenario, the SSP119 scenario consumes the least amount of energy for air-conditioning with the associated GHG emissions peaking in 2035, generating less than half of the baseline GHG emissions in 2050.

Our findings show that there are substantial differences in AC-related emissions across scenarios, with the drivers of GHG emissions

changing from electricity consumption to the leakage of air-conditioning refrigerants (see Fig. 3b). Global cumulative GHGs from AC use (see Fig. 3c) would reach 113.3 (83.8–168.7) GtCO₂eq between 2010 and 2050 under the baseline scenario. China and the United States alone account for almost 40% of annual emissions from AC use by 2050 across all scenarios, equivalent to the total emissions of the other top ten regions. Among all AC-related GHG emissions, refrigerant leakage is projected to become the primary source by 2050, accounting for up to 60% of total AC-related GHG emissions. The joint influence of global warming and socio-economic development markedly extends the working hours and operating units for air-conditioning. GHG emissions from electricity use and refrigerant leakage would correspondingly increase⁴⁴. Decarbonization in power supply structure could offset some of these emissions. Deployment of renewable energy and negative-emission technologies restrains CO₂ emissions from both residential and commercial cooling sectors between 2010 and 2050: under the SSP585 scenario, annual CO₂ growth is limited to 3.1% and 3.4%, respectively, whereas under the most stringent scenario (SSP119), 2050 emissions fall below 2010 levels by 27.4% and 25.0%. By contrast, the shift to low-GWP refrigerants is progressing far more slowly, allowing non-CO₂ GHGs from AC use to grow at more than twice the CO₂ rate, sustaining annual increases of about 3%–7% across scenarios.

GHG emissions from AC use, in turn, would result in additional global-mean temperature increases by 2050, ranging from 0.02 °C (the lower bound for the SSP119 scenario) to 0.11 °C (the upper bound for the SSP585 scenario) across the five SSP-RCP scenarios. Under the baseline scenario, there would be an additional 0.05 °C (0.03 °C–0.07 °C) temperature increase by 2050. The SSP585 scenario produces the most cumulative GHG emissions from AC use with the highest warming impact, bringing about an additional 0.07 °C (0.05 °C–0.11 °C) temperature increase by 2050. In comparison, the SSP119 scenario would only see an additional temperature increase of 0.03 °C (0.02 °C–0.04 °C). Given that the observed warming from 1998 to 2012 is about 0.05 °C (–0.05 °C–0.15 °C) per decade^{45,46}, this additional impact could accelerate global warming, reducing the likelihood of achieving the 1.5 °C or 2 °C temperature targets. Historical data further underscores the escalating economic damage associated with natural disasters under such warming conditions: the economic loss from the top 1% of single-event disasters reached 9.92 billion USD in 2010, more than doubling since 1998⁴⁷. Economic ramifications of this additional warming in production are far-reaching, indicating that global output could drop 2.5% in response to a temporary increase of 1 °C⁴⁸.

The total warming impact from AC use is attributable to the combined effects of socio-economic development and a climate-driven feedback loop. The socio-economic component captures the fundamental growth in cooling demand through population growth and rising affluence. The climate-driven warming feedback, in contrast, captures the additional, self-reinforcing loop that occurs as rising temperatures necessitate more cooling, which in turn generates more emissions. To separate global warming from socio-economic development, we construct a simplified counterfactual scenario analysis by fixing regional CDDs at their 2010-level on all future years to quantify their respective contributions of warming impact (see Supplementary Tables 7 to 11). Removing the climate-warming signal systematically lowers projected AC energy demand and the attendant GHG emissions in every scenario, with the gap widening over time. The climate-driven feedback is projected to cause no more than 0.01 °C of additional warming by 2050 across all five SSP-RCP scenarios. In line with our previous analysis, socio-economic development dominates the additional warming impact from global AC use. For example, the climate-driven feedback peaks at about 0.01 °C under the most warming scenario (SSP585), indicating that socio-economic development contributes –0.06 °C of warming. In contrast, under the lowest-warming SSP119 scenario, the differences between the two drivers are the

greatest: the climate-driven feedback is projected to reach only 0.001 °C, while the contribution from socio-economic development is projected to be more than 0.03 °C.

Therefore, achieving a low-carbon transition is critical to mitigating the total warming impact associated with AC use. Such a transition not only suppresses the climate-driven warming feedback by slowing global warming itself, but also enables socio-economic development to proceed with substantially mitigated emissions through the deployment of clean energy supplies. Our results show that increased AC usage is projected to cause an average 101.7% increase of global direct cooling emissions from AC use between 2010 and 2050 (see Supplementary Table 5 to 6). Mitigation policies effectively drive the low-carbon transition of the power sector, particularly under the SSP119 scenario, achieving a 75.1% reduction in CO₂ emissions. In contrast, the non-CO₂ emission intensity effect results in increased non-CO₂ emissions across all scenarios, indicating that the current low-GWP refrigerant transition is progressing slowly. Regional patterns, however, diverge sharply. In high-income regions with a high adoption of efficient, low-GWP refrigerants (e.g., the United States), the non-CO₂ emission intensity effect contributes to over 90% of the emission reductions under low-emission scenarios. However, in regions with rapid growth in AC demand that primarily use high-GWP refrigerants (e.g., China), it contributes to a 362.1% increase in non-CO₂ emissions even under the SSP119 scenario, –1.6 times greater than the energy use effect.

Global inequality in the use of air-conditioning

Socio-economic development, especially household income, stands as the most important driver of global AC energy demand and the resulting GHG emissions. This means the profound global income disparities inevitably create a deeply unequal distribution of cooling access and its associated burdens. Although income growth from 2010 to 2050 reduces inequality in both cooling energy demand and expenditure, inequality remains high even after accounting for differences in regional cooling demand (CDD-adjusted Gini; Fig. 4). Higher income growth expands access to thermal comfort and narrows global inequalities in AC use, but they also increase global AC stock, as well as the associated energy consumption and GHG emissions. To further quantify the influence of rising incomes on global AC use, we employ an econometric model to estimate income-driven cooling gaps under three income-adjusted scenarios (see Fig. 5). Here, cooling gaps represent the difference between previously estimated AC stock under SSP-RCP scenarios and AC stock estimated derived from corresponding income-adjusted scenarios. Specifically, we build medium-income, high-income, and maximum-income scenarios within each SSP-RCP framework: raising the income of (1) populations in low-income regions to the average income of middle-income regions; (2) populations in low- and middle-income regions to the average income of high-income regions; (3) populations across all regions to the highest income level under the corresponding SSP-RCP scenario. Our results indicate that raising household incomes in low-income regions would increase the global AC stock by –one million units and increase the operating hours by at least 40% by 2050. If all regions achieved the highest income level envisioned in each SSP framework, global AC stock would expand by tens of millions of units, driving an extra 0.003 °C–0.05 °C increase of global-mean temperatures even under the most stringent SSP119 scenario.

All Lorenz curves are constructed by ranking regions from lowest to highest per-capita GDP, allowing direct comparison with global economic inequality, following Zhao et al.⁴⁹. Although the ratio of per-capita GDP by 2050 between the highest-income 10% and the lowest-income 10% of the global population remains larger than the corresponding ratio for energy consumption and expenditure for cooling. However, this conceals deeper, underlying inequalities. Based on the Gini coefficients, the distribution of energy consumption and

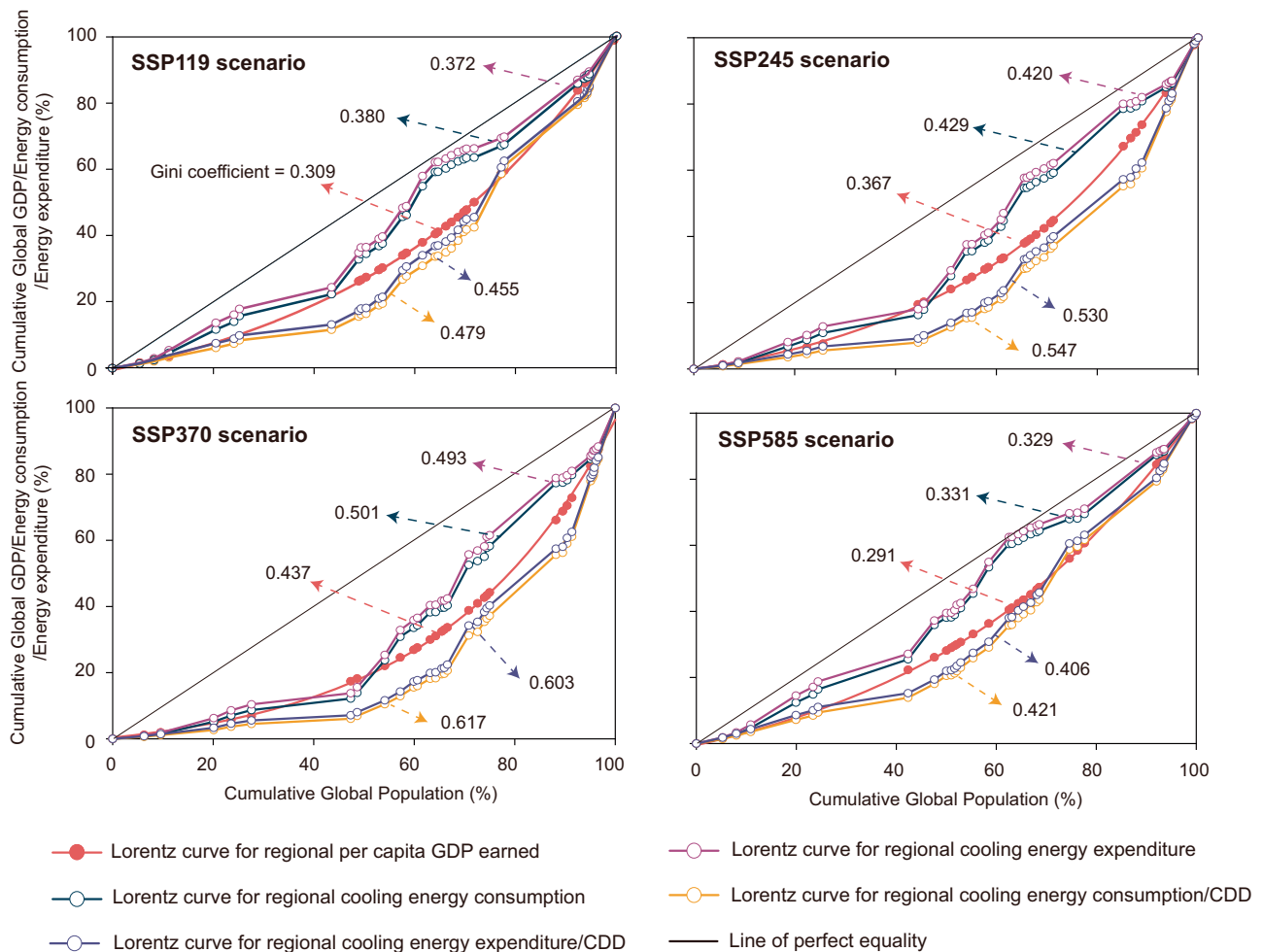


Fig. 4 | Lorenz curves for regional energy consumption and expenditure for cooling. Lorenz curves for cooling energy consumption and expenditure attributable to per capita GDP (in 1990 US \$ Purchasing Power Parity prices) at the global level in 2050 under the SSP119, SSP245, SSP370, and SSP585 scenarios. See Supplementary Fig. 4 for the SSP126 scenario. The yellow Lorenz curve represents global economic inequality, with data points ordered by per capita income of

GCAM regions from low to high. To facilitate a direct comparison with economic inequality, we use the same regional ordering for the other Lorenz curves to illustrate the difference between global distribution of income and the distribution of cooling energy consumption and expenditure (see “Methods”). Gini coefficients of GDP, cooling energy consumption and cooling energy expenditure across all scenarios are shown in Supplementary Table 7.

expenditure for cooling is more unequal than GDP. Income growth helps to narrow these gaps. Based on SSP narratives, global economic inequality declines by 2050 in all scenarios, with the Gini coefficient shifting from high inequality towards less than 0.4 in 2050 (except for the SSP370 scenario, see Supplementary Table 12). As a result, the Gini coefficient for cooling energy consumption decreases to 0.47 and the Gini coefficients for cooling expenditure declines to 0.45 in 2050 under the baseline scenario. The lowest-income 10% of the population would consume about 2% of global cooling energy in 2050 and are linked to 3% of global cooling expenditure. In comparison, the highest-income 10% of the global population could have access to cheaper cooling service than the lowest-income 10% of the population, consuming around 18% of global cooling energy linked to 17% of global cooling expenditure. Scenario differences further reinforce this pattern. The SSP585 scenario, which features the highest income growth, has the most equal distribution of energy use and expenditure for cooling among the five scenarios. The highest-income 10% of the global population is expected to consume ~4 and 3 times more cooling energy and expenditure than the lowest-income 10% in 2050, with these differences being substantially lower than those observed in the baseline scenario. In contrast, the SSP370 scenario, characterized by slow and uneven economic development, shows the most unequal

distribution, with the differences in cooling energy use and expenditure between the highest-income 10% and the lowest-income 10% projected to increase to 13- and 10-fold, respectively. Under low-emission scenarios, higher mitigation costs result in higher unit cost of cooling services relative to the other scenarios, which does not make cooling service more affordable for low-income people. Thus, achieving low-carbon targets contributes little to narrowing differences in energy use and expenditure for cooling relative to the SSP585 scenario.

However, such regional differences in energy use and expenditure for cooling become even more pronounced if regional differences in cooling demand are considered. Many high-income regions are located in high-latitude areas, where climate characteristics result in relatively low cooling energy consumption and expenditure. This geographic mismatch between cooling demand and economic development can obscure differences in cooling energy consumption and expenditure per unit of cooling demand. When we normalize by regional cooling demand, inequality intensifies. Specifically, under the baseline scenario, the differences in cooling energy consumption and expenditure per CDD between the highest-income 10% and the lowest-income 10% increase from 6- and 5-fold (without considering regional cooling demand differences) to 20- and 15-fold, respectively. Such

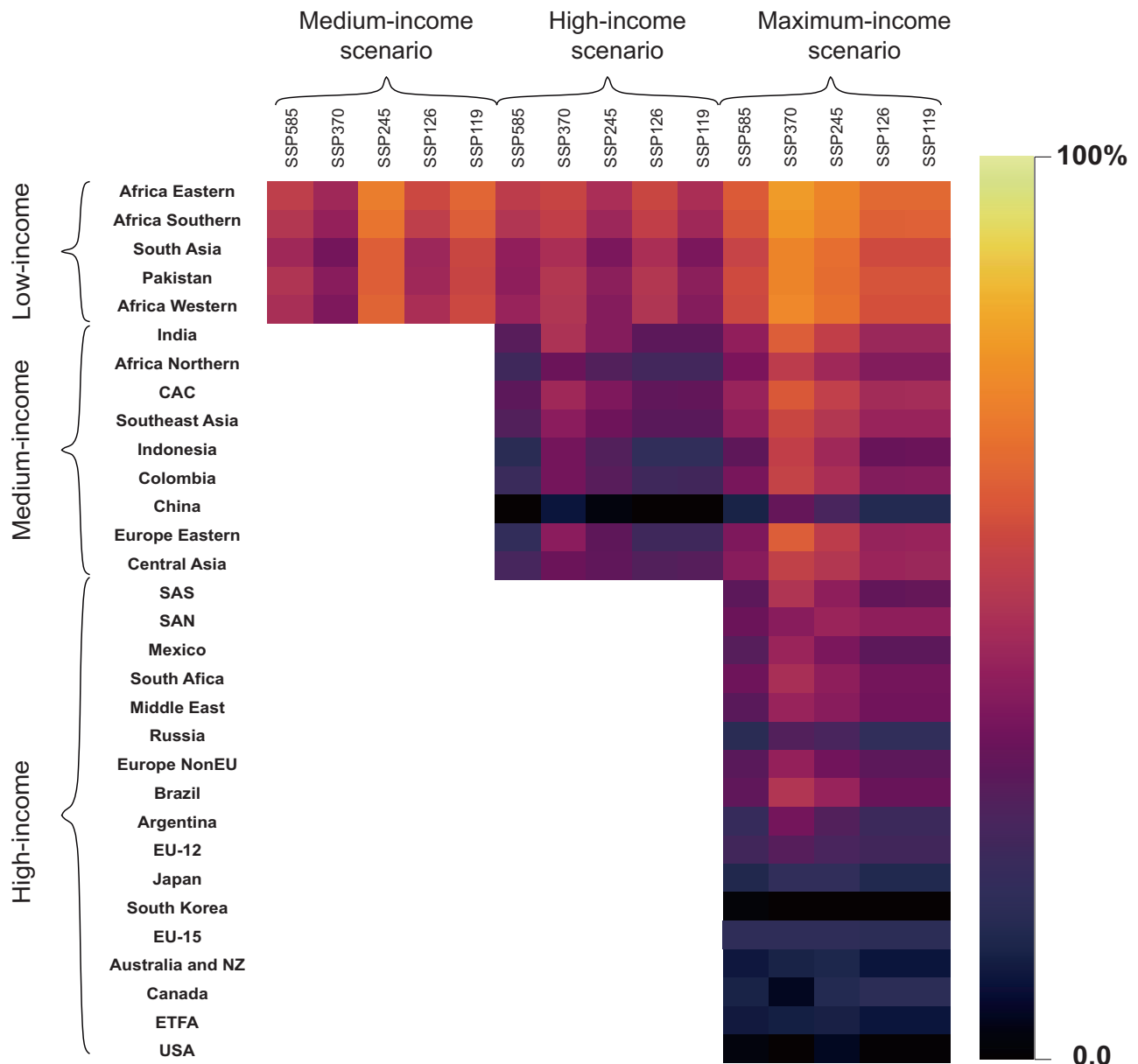


Fig. 5 | Regional cooling gaps across SSP-RCP scenarios. We have divided GCAM regions into three income groups, i.e., low-income, medium-income and high-income, based on the World Bank definition in 2015⁸² and van Ruijven, et al.⁸³ (details shown in Supplementary Information). The shading represents the proportion of cooling gaps to total AC stock for the corresponding income level within

the SSP-RCP scenarios. A higher proportion indicates a greater potential increase in air-conditioning units following an income rise in the region. CAC, SAS, SAN and ETFA represent Central America and Caribbean, Northern part of South America, Southern part of South America and European Free Trade Association regions, respectively.

differences are most pronounced under the SSP370 scenario, reaching -8- and 29-fold in 2050, respectively. These results indicate that, relative to their climatic requirements, the lowest-income populations consume far less cooling energy than the highest-income populations, highlighting a substantial inequality in access to cooling services.

Higher incomes dramatically accelerate the expansion of the installed AC stock, yet regional differences in the underlying cooling-demand modulate the scale of that growth. For example, regions with low climatic cooling demand tend to not require air conditioners even at high income levels. Canada is projected to have similar population size and per capita income to South Korea in 2050 across scenarios, while its average AC stock are projected to be -14% of South Korea's. That is because higher air temperature and relative humidity in summer would result in far greater demand for air conditioners in South Korea relative to Canada. We adopt the ratio of cooling gaps to the

projected AC stock under corresponding income-adjusted scenarios to quantify the extent of inequalities in global AC stock. We find that cooling gaps would reach 94 (86-111) million units in 2050 for low-income regions, equivalent to ~45% of total AC stock under the medium-income scenarios. Income constraints on AC stock are the most pronounced under the SSP370 scenario, where its corresponding projected amounts of AC use can only meet 50% of those required for a medium-income lifestyle in low-income regions. Furthermore, cooling gaps under the high-income scenario would respectively reach 150 (126-166) and 117 (55-176) million units in 2050 for low-income and medium-income regions, equivalent to 56% and 27% of their income-adjusted AC stock. Most importantly, assuming that cooling access across regions were to become the same as the highest-income regions, global cooling gap in 2050 would increase to 0.7-1.1 billion units.

Accounting for the increased working hours of AC devices, income-adjusted scenarios are projected to drive a substantial surge in AC-related GHG emissions. We treat the income-induced change in unit energy consumption (see section 4 in SI) as a proxy for increased operating hours. Using the most stringent SSP119 scenario as an example, the cumulative GHG emissions between 2010 and 2050 are projected to increase by 19.1% under the medium-income scenario. Under the high-income scenario, cumulative AC-related GHG emissions from low- and medium-income regions are projected to increase by 107 GtCO₂eq each, exceeding the total AC-related emissions projected for the SSP126 scenario. Compared to the warming impact from the SSP119 scenario, additional GHG emissions under the medium-income scenario would cause an additional 0.003 °C increase of global-mean temperatures, while a respective additional 0.015 °C of warming under the high-income scenario. Under the maximum-income scenario, the cumulative GHG emissions between 2010 and 2050 would have a roughly 2-fold increase, surpassing the totals projected under the SSP585 scenario, with a further increase in temperature of 0.05 °C.

Discussion

Across the five SSP-RCP scenarios, global air-conditioning use is projected to raise global-mean temperature by 0.03 °C–0.07 °C by 2050, indicating that increasing AC use further exacerbates climate change. Most of this total warming impact (0.03 °C–0.06 °C) reflects the socio-economic warming contribution, whereas the climate-driven warming feedback remains below 0.01 °C in all pathways, which is small but not negligible. These estimates underscore the critical need to address the energy-emissions-temperature impact associated with AC use, which not only imposes billions of dollars in economic loss⁴⁸ but also accelerates global warming and further makes achieving the Paris Agreement goals more difficult⁵⁰. However, the actual impact may be even more severe. First, our findings are likely conservative, as they are derived from a one-way evaluation under varying climate conditions. In an ideal scenario, GCMs would capture the additional warming effects induced by AC use, as well as the heat-island effects associated with cooling systems^{51,52}, thereby informing new estimates of regional cooling demand under elevated temperature conditions, enabling these insights to be integrated into IAMs and ultimately facilitating a continuously iterative modeling framework. However, such an approach requires extensive computational resources, sophisticated model calibration, and extensive interdisciplinary collaboration⁵³. This warming potential would likely reveal greater increases in cooling demand and associated emissions^{54,55}, indicating that the present analysis underestimates the full extent of these impacts. Second, this study focuses exclusively on air-conditioning as the primary cooling technology due to limitations in modeling capabilities and data accessibility. This means that our study does not represent the heterogeneity of potential or available cooling devices and does not provide insights on the potential of adaptation, including the use of alternative forms of cooling with lower (or higher) energy efficiency, causing uncertainties in cooling-related energy consumption and emissions. For example, while fans can reduce energy consumption by 76% compared to AC for the same cooling effect⁵⁶, other studies suggest that fan energy consumption is still substantial, potentially accounting for around 1.5% of TEC in the building sector globally in 2016⁴. As a result, our analysis likely underestimates the extent of the resulting warming impact but also ignores low energy-intensive alternatives.

Moreover, our study shows that reducing the total warming impact from AC use demands immediate implementation of targeted mitigation measures, particularly accelerated power sector decarbonization and widespread adoption of low-GWP refrigerants. Cooling-related electricity consumption is estimated to be -3600–12,821 TWh in 2050 across scenarios, accounting for 13%–47% of global total electricity

consumption in 2022. A high share of renewable energy systems could substantially reduce or eliminate the emissions associated with increased AC-related electricity. Similarly, transitioning to low-GWP refrigerants has a direct climate impact on AC systems themselves. For example, our results estimate low-GWP refrigerants, such as HFC-32, would comprise 25% of all refrigerants by 2050 under the SSP119 scenario, resulting in 84% lower emissions compared to the SSP585 scenario. Thus, when legislation is more stringent, adopting more efficient and low-GWP refrigerants, such as R-290 and R-1234yf, in place of HFC-134a could contribute up to 90–99% emission reduction⁵⁷. In addition, building retrofits represent critical strategies for reducing cooling energy consumption, particularly in regions with high cooling demands. Evidence shows that building retrofits, such as using aerogels to improve insulation⁵⁸ and retrofit double glazing⁵⁹, can reduce annual cooling energy consumption by 7.5% in tropical regions. Providing subsidies for the adoption of energy-saving equipment can also improve the efficiency of cooling systems in buildings⁶⁰. Studies show that the large-scale application of air-to-air heat pumps in the USA could provide 5%–9% emission reduction based on the current power system⁶¹. The strategies discussed above require substantial economic investment and extended timeframes, making it challenging to deliver short-term impacts. Behavioral changes driven by policy interventions could play a critical role in achieving short-term reductions in AC energy consumption⁶². For example, dynamic pricing strategies that raise electricity costs during peak hours and temperature adjustment policies that increase cooling setpoints during peak demand periods can incentivize users to shift their cooling demand to off-peak times, potentially reducing peak electricity loads by up to 20%⁶³. Additionally, environmental education campaigns can promote energy-saving habits among the public, such as setting thermostats at optimal levels or adopting passive cooling strategies⁶⁴, bringing about 6%–20% energy-savings from AC use⁶⁵.

Our analysis of global inequalities in the use of air-conditioning uncovers a fundamental development dilemma: low income considerably limits regional access to cooling, yet closing this gap to deliver equitable thermal comfort would generate substantial additional warming impact. Gini coefficients demonstrate that, once regional cooling demand is considered, disparities in cooling services far exceed those implied by income alone. The effect arises from a stark geographic mismatch between cooling demand and economic development, which greatly amplifies income-based inequality. Our analysis quantifies the potential increase in global AC demand resulting from rising incomes in low-income regions: an additional 94 million units at medium-income levels, 150 million units at high-income levels, and up to over 220 million units at the highest-income levels. Incorporating total AC stock expansions and extended usage durations, our estimates project additional GHG emissions that would induce an additional 0.003 °C–0.05 °C of warming even under the SSP119 scenario, highlighting the trade-offs between equitable cooling access and additional warming impact. Moreover, achieving low-emission pathways would not notably reduce the inequalities in AC use compared to the high-emission pathway. High unit costs of cooling due to stringent mitigation policies may make cooling services less affordable for lower-income populations, potentially exacerbating existing inequalities and undermining the goals of a 'just energy transition'. While ambitious climate mitigation itself reduces cooling gaps and potential contribution to global warming, targeted cooling policies are required to close regional differences in cooling gaps. Therefore, it is urgent to accelerate a green and sustainable transition while promoting inclusive development.

Methods

Integrated assessment framework

This study develops an integrated assessment framework to quantify the total warming impact and inequalities resulting from AC use under

various climate scenarios (see Fig. 6). For this scenario analysis, we utilize the SSP-RCP framework to simulate climate scenarios, matching the outputs of multiple GCM models from the CMIP6 database (see the Climate scenarios section). Subsequently, we quantify global and regional cooling demand across different scenarios using an improved population-weighted CDD approach, incorporating the heat-index approach (see the heat-index approach section). We integrate the improved regional CDDs as climate inputs into a widely used integrated assessment model GCAM^{19,66}, enhancing the ability to project future AC energy consumption and associated GHG emissions. Additionally, by assessing AC-related impacts within GCAM across five IPCC-endorsed SSP-RCP scenarios, our findings provide a comprehensive outlook on future AC energy use and emissions under possible ranges of global warming trajectories and socio-economic development. Lastly, we assess the inequality in the use of air-conditioning using Gini coefficients and quantify the cooling gaps with an econometric model. The formulas used for the inequality assessment are presented below, with additional robustness analysis for the econometric model provided in the Supplementary Information. Finally, we employ the MAGICC model to evaluate the additional warming effects resulting from the GHG emissions associated with AC use. Detailed information is provided at the end of the “Methods” section.

Climate scenarios

In our research, we select five scenarios (SSP119, SSP126, SSP245, SSP370 and SSP585), combining Shared Socio-economic Pathways (SSPs) with Representative Concentration Pathways (RCPs) to depict future climate change scenarios. SSPs are narratives that describe plausible future global developments in demographics, economics, technology, and environmental factors without considering climate change or mitigation policies⁶⁷. Each SSP outlines different challenges to mitigation and adaptation²⁹: sustainable development (SSP1), middle of the road (SSP2), regional rivalry (SSP3), inequality (SSP4) and fossil-fueled development (SSP5). RCPs represent trajectories of GHGs and other forcing agents to guide modeling potential climate outcomes. The original RCP scenarios include four scenarios: RCP2.6 (very low forcing scenario), RCP4.5 and RCP6.0 (medium stabilization levels), RCP8.5 (a very high emission scenario)³⁰. In the IPCC AR6^{23,24}, two additional scenarios, RCP1.9 and RCP7.0, were introduced, representing global 1.5°C pathway and a high-emission baseline scenario, respectively. These five selected scenarios cover a wide range of possible climate outcomes and anthropogenic emissions pathways, and thereby encapsulate the uncertainties and complexities of projecting long-term climate and societal changes. Additionally, by using the same SSP-RCP scenarios recommended by the IPCC AR6, we ensure that our study is aligned with the global GCM community, strengthening the robustness of our findings. The main assumptions and warming outcomes of the SSP-RCP scenarios are shown in Supplementary Table 8. We acknowledge that the SSP4 scenario, which focuses on unequal development, is not included in our choice of five illustrative scenarios, meaning that the scenario characterized by significant inequalities in AC use has not been explicitly explored. However, even in the absence of SSP4, our analysis still captures key contrasts in inequalities between SSP3 (high inequality, high vulnerability) and SSP1 (low inequality, high resilience). While the inclusion of SSP4 may provide additional valuable insights, its exclusion does not diminish the broader relevance or robustness of our findings.

Heat-index approach

The heat-index approach, developed by Lans P. Rothfusz and Steadman (https://www.wpc.ncep.noaa.gov/html/heatindex_equation.shtml), is widely used to capture the impacts of RH on regional

thermal comfort levels^{68–70}. We introduce the heat-index approach to extend the Cooling Degree Days approach by combining both air temperature and humidity, which is a prerequisite to accurately measure the cooling demand of each GCAM region. Existing studies have demonstrated that RH affects the value of perceived temperature a lot but have often been ignored in the long-term climate change modeling³⁶. Based on the daily gridded data of near-surface air temperature and RH from the CMIP6 database and the NASA NEX-GDDP-CMIP6 database across SSP-RCP scenarios, we calculate the heat index in each grid for distinct conditions: temperatures below 80 °F, temperatures above 80 °F, RH below 13% with temperatures between 80 °F and 112 °F, and RH above 85% with temperatures between 80 °F and 87 °F. When the temperature is below 80 °F, the Rothfusz regression model is deemed unsuitable, as it has not been validated for lower heat index values. We use a simplified function (Eq. (1)) to provide a reasonable approximation of the heat index at lower temperatures, where extreme heat stress is less of a concern:

$$HI_{below\ 80^{\circ}F} = 0.5 \times \{T + 61.0 + [(T - 68.0) \times 12] + (RH \times 0.094)\} \quad (1)$$

Where HI represents the heat index value, also called the apparent temperature adjusted by relative humidity; T represents the near-surface air temperature in degrees F; and RH represents relative humidity in percent.

For temperatures exceeding 80 °F, we utilize a multiple regression model developed by Lans Rothfusz (Eq. (2)), which was specifically designed to accurately model heat index values under high temperature and humidity conditions:

$$\begin{aligned} HI_{above\ 80^{\circ}F} = & -42.379 + 2.04901523 \times T + 10.14333127 \times RH \\ & - 0.22475541 \times T \times RH - 0.00683783 \times T \times T \\ & - 0.05481717 \times RH^2 + 0.00122874 \times T^2 \times RH \\ & + 0.00085282 \times T \times RH^2 - 0.00000199 \times T^2 \times RH^2 \end{aligned} \quad (2)$$

Furthermore, when RH is below 13% with temperatures between 80 °F and 112 °F, a reduction adjustment is applied to account for the diminished perceived heat due to dry air:

$$Adjustment = [(13 - RH)/4] \times \sqrt{[17 - |T - 95|]/17} \quad (3)$$

Conversely, when RH exceeds 85% with temperatures between 80 °F and 87 °F, an increase adjustment is added to reflect the heightened perception of heat in humid conditions:

$$Adjustment = [(RH - 85)/10] \times [(87 - T)/5] \quad (4)$$

After the above steps, the heat index value represents the apparent temperature in each grid, which is used as the air temperature inputs for the Cooling Degree Days approach.

Population-weighted cooling degree days approach

Cooling Degree Days approach is widely used to measure the extent to which air-conditioning cooling could be required for a given period of time^{70,71}. We have extended the Cooling Degree Days approach to the population-weighted Cooling Degree Days by taking into account both the apparent temperature adjusted by heat-index approach and future population distribution. The population distribution projections along the SSP framework comes from Socioeconomic Data and Applications Center (SEDAC database)³². Accordingly, population-weighted Cooling Degree Days approach provides more accurate projections of regional cooling demand for air conditioning under different future climate change and socioeconomic scenarios, contributing to a better

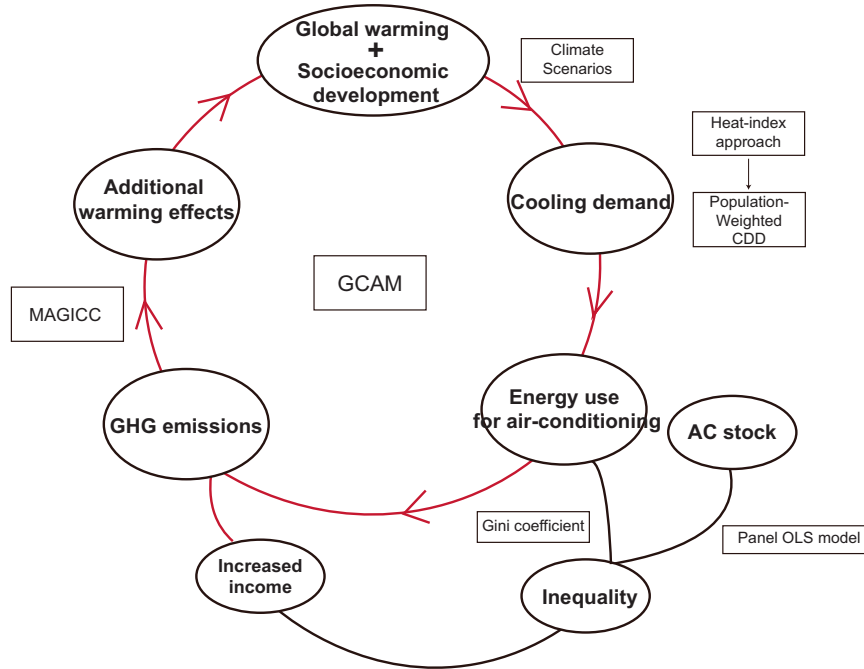


Fig. 6 | Research framework of this study. The red circle represents the total warming impact from AC use. The content within the ellipse represents the key steps and components of the comprehensive assessment of air-conditioning, while

the content within the boxes outlines the key methodologies employed to achieve the main objectives of this study.

understand the impacts of climate change on different regions. Population-weighted CDDs for 32 regions defined in GCAM is calculated using the following equations.

$$CDD_{i,j}^{day} = \max(T_{i,j}^{mean,day} - T_{i,j}^{base,day}, 0) \quad (5)$$

Where, i represents GCAM region i ; j represents the grid cell j ; $CDD_{i,j}^{day}$ represents daily cooling degree days in grid cell j of region i ; $T_{i,j}^{mean,day}$ represents the daily heat index value in grid cell j of region i ; $T_{i,j}^{base,day}$ represents a given point (18 °C in this paper based on numerous global CDD studies^{17,36,72}), which is used for measuring the amount and duration of temperature being above this point. This choice is still a topic of considerable discussion for long-term global assessments. One limitation is that a uniform base temperature may not fully capture regional variations in thermal comfort thresholds, while this simplification facilitates global comparisons (see Limitations). Moreover, our choice of base temperature does not account for the influence of RH, which may create a degree of inconsistency with the heat-index approach. However, incorporating RH into the baseline temperature would introduce seasonal and regional variations, making global CDD aggregation and comparison less uniform and more complex. The current compromise strikes a balance between the need for regional specificity in the heat index approach and the practicality of calculating CDDs using a standardized baseline temperature. Furthermore, we conducted a sensitivity analysis using various base temperatures (see Supplementary Fig. 5) to quantify the impact of this parameter choice. While the results demonstrate considerable sensitivity of absolute CDD magnitudes to the selected base temperature, employing a consistent 18 °C base temperature is crucial for maintaining comparability when assessing relative CDD trends across diverse regions and scenarios.

$$CDD_{i,j}^{year} = \sum_{day} CDD_{i,j}^{day} \quad (6)$$

Where $CDD_{i,j}^{year}$ represents yearly cooling degree days in grid cell j of region i after adding up all daily cooling degree days.

$$CDD_i^{population-weighted, year} = \frac{\sum_j CDD_{i,j}^{year} \times Pop_{i,j}^{year}}{\sum_j Pop_{i,j}^{year}} \quad (7)$$

Where $CDD_{i,j}^{population-weighted, year}$ represents population-weighted CDDs of region i ; $Pop_{i,j}^{year}$ represents the population amount in grid cell j of region i .

Global change analysis model (GCAM)

GCAM model is an open-source integrated assessment model, providing long-term simulation of economic, energy, land use, water resources and climate change interactions at global and regional levels¹⁹. In this study, we use GCAM model in its widely used version of 5.2¹⁸ to match the same base year (2010) of climate outputs from 25 GCMs. Within GCAM, the world is divided into 32 energy-economic regions, simulating the equilibrium prices and quantities of various energy and GHG markets in each time period and in each region in five-year time steps from 2010 to 2100. Population and GDP are specified as exogenous parameters to drive a range of demand sectors in GCAM, aligned with the SSP narratives in our research. RCP scenarios are implemented by setting climate constraints or targets for designed years, with GCAM dynamically adjusting carbon prices to identify the least-cost pathway to meet climate goals.

In the GCAM, the effects of climate change on cooling expenditures and energy consumption for air-conditioning are estimated within the building sector modeling, accounting for improvements in air-conditioning efficiency and building energy efficiency (see details in ref. 17). Specifically, rates of shell conductivity improvements are set at 0.5% per year for industrialized countries and 0.8% per year for medium- and low-income regions, while AC technologies improve at rates ranging from 0.25% per year in industrialized countries to 0.58%

per year in medium- and low-income regions over the century¹⁷. Cooling technologies in GCAM encompass various air-conditioning cooling technologies but exclude other methods such as fans.

As shown in Eq. (8), per capita expenditures for cooling (E_t) are mainly driven by the leveled cost of the cooling services per unit floorspace in period t (P_t) and the per-capita energy consumption of cooling services (C_t). For convenience, it is useful to decompose C_t into floorspace per capita (f_t), and the energy consumption of cooling services per unit of floorspace (c_t).

$$E_t = C_t P_t = f_t c_t P_t \quad (8)$$

The demand for floorspace per capita is shown below.

$$f_t = (s - a) \times \left[1 - \exp\left(-\frac{\ln(2)}{\mu} \times I_t \times \left(\frac{P_t}{P_{t0}}\right)^\beta\right) \right] + a \quad (9)$$

Where f_t shows future demand for per-capita floorspace in future time period t ; s is the exogenous satiation level of per-capita floorspace, set to different values under various SSP scenarios, indicating the level of service demand at which increases in income do not lead to further demands for services; μ is the per-capita GDP at 50% of the satiation level, β is the price elasticity of floorspace demand; a is an exogenous tuning parameter, P_t is the total leveled cost of the modeled energy services per unit floorspace in period t , t_0 is the base year, and I_t is per capita GDP in period t .

In modeling cooling energy consumption (Eq. (10)), GCAM and other IAMs share a focus on incorporating climatic variables, building characteristics, and socioeconomic factors⁷³, yet they differ in approach and assumptions^{73,74}. GCAM features an endogenous, bottom-up building sector that directly models these influences within a single framework, while other IAMs, such as AIM-Hub⁷⁵ and MESSAGEix⁴¹ models, tend to rely on multi-model coupling and AC adoption assumptions to represent cooling energy demand. Additionally, the modeling structure also influences cooling energy consumption. For example, general equilibrium models, compared to partial equilibrium models, account for costs imposed by other sectors, often leading to higher costs and lower energy demand⁷⁵.

$$c_t = k \times (CDD_t \times \eta_t \times R_t + \lambda_c \times IG_t) \left[1 - \exp\left(-\frac{\ln(2)}{\mu} \frac{I_t}{P_t}\right) \right] \quad (10)$$

Where in period t , c_t represents the demand of cooling services, CDD_t shows global population-weighted CDDs; η_t is the exogenous average building shell conductance, R_t is the exogenous average floor-to-surface ratio of buildings, IG_t is the internal gain heat from other building services, and λ_c is an exogenous internal gain scaler.

On the basis of energy consumption for air-conditioning, we further calculate GHG emissions from AC use across regions. Energy-related GHG emissions, including CO₂ emissions from electricity use and non-CO₂ emissions from power transmission, are calculated based on different emission factors. The emission factors of power grid are derived by the amount of electricity generated each year and the associated emissions from GCAM model. Non-energy related GHG emissions from AC use, such as various AC refrigerants (C₂F₆, HFC134a, HFC143a, HFC32), are modeled in detail through various air-conditioning technologies for cooling in the GCAM (see details in <http://jgcri.github.io/gcam-doc/v5.2/emissions.html>). Additionally, given that the range of CDD values (maximum, mean, and minimum) derived from 25 GCM models under each SSP-RCP scenario, the energy consumption and emissions from air conditioning also exhibit corresponding ranges, thereby reducing uncertainty in the results. Global energy demand for air-conditioning during 2015-2050 across five SSP-RCP scenarios is shown in Supplementary Table 9.

Lorenz curve and Gini coefficient for inequality assessment of AC use

The Lorenz curve provides a graphical representation of income or wealth inequality within a population. It is typically depicted with the cumulative share of income or wealth (%) on the vertical axis, and the cumulative share of the population (%), ranked from lowest to highest income) on the horizontal axis. The Gini coefficient, a numerical measure of inequality derived from the Lorenz curve, ranges from 0 (perfect equality) to 1 (perfect inequality). The basic income Gini coefficient is calculated using the following formula:

$$G = 1 - \sum_{i=1}^n (P_{i+1} - P_i)(Y_i + Y_{i+1}) \quad (11)$$

Where G refers to economic development Gini coefficient, P_i is the cumulative share of population of region i , Y_i is the cumulative share of GDP of regional i , and n is the number of regions. We rank the regions according to their GDP per capita to show the inequalities in economic development.

Here, we also apply the Lorenz curve to assess the inequality in cooling energy consumption and expenditure across different regions, based on data obtained from the GCAM under the five SSP-RCP scenarios. The analysis was based on key indicators derived from GCAM: cooling energy consumption, cooling energy expenditure, cooling energy consumption per CDD, and cooling energy expenditure per CDD. And following the method in Zhao et al.⁴⁹, we use the same per-capita GDP ranking order for the other Lorenz curves to compare the inequality in economic development with the inequality in the use of air-conditioning.

Empirical approach for future AC stock and quantifying the unmet income-driven cooling needs

We develop a reduced form of econometric model to forecast the number of AC units in use under a given scenario. The response function of AC stock is estimated for each region by applying panel Ordinary Least Squares (OLS) in logarithmic form. Following previous work from Diffenbaugh and Burke⁷⁶, Davis, et al.³⁸ and Colelli, et al.⁴², AC stock are determined as a function of CDDs, incomes, and urbanization rates. We adopt CDDs and the quadratic term of CDDs to capture the impacts of global warming on AC demand. Per capita GDP represents the regions' income, and the proportion of urban population represents the urbanization rates. The region and year fixed effect estimation allows us to control for time-invariant and time-varying unobservable region characteristics that may be correlated to air condition demand. The empirical model takes the following form:

$$\ln \overline{AC}_{it} = \alpha_0 + \beta_1 \ln CDD_{it} + \beta_2 (\ln CDD_{it})^2 + \beta_3 \ln income_{it} + \beta_4 \ln urbanization_{it} + \beta_5 \ln pop_{it} + \lambda_i + \delta_t + \varepsilon_{it} \quad (12)$$

where i and t represent the region and year, respectively; dependent variable $\ln \overline{AC}_{it}$ is the natural logarithm of AC demand; $income_{it}$ is per capita GDP; $urbanization_{it}$ is urbanization rate of each GCAM regions; pop_{it} is population of GCAM region i in period t . To avoid the effect of different scales of variables, we add 1 to all the variables and then take the natural logarithm. To mitigate the potential bias induced by outliers within the dataset, we employed a winsorizing procedure at the 1% and 99% distribution tails, replacing extreme observations with the corresponding values identified at these percentiles. Hence, the actual air-conditioning stock are estimated as follows:

$$AC_{it} = e^{\ln \overline{AC}_{it}} - 1 \quad (13)$$

We estimate the coefficients of each variable based on data from 1990-2014. Furthermore, utilizing these coefficients as pivotal parameters, the forecast value of logarithmic value $\ln \overline{AC}_{it}$ of the demand for air conditioning is estimated based on the future CDDs, incomes

and urbanization rates. Moreover, we have conducted robust analysis and regional heterogeneity analysis to ensure the reliability and uncertainties of our results (see Supplementary Fig. 6, Supplementary Table 10 to 11).

Model for the Assessment of Greenhouse Gas Induced Climate Change (MAGICC)

Since long-term climate impacts depend on cumulative GHG emissions from AC use, we employ the climate emulator MAGICC in its version 7.5.3, which is the same version and calibration that was used by Working Group III of the IPCC Sixth Assessment Report^{24,77}. MAGICC, a reduced complexity earth system model, is widely recognized for its satisfactorily representation of the global warming response to emissions. Numerous studies have validated its bias and precision, particularly for global-mean temperature estimates, in comparison to more complex climate models^{77,78}. In our study, we set the climate sensitivity of the MAGICC model to 3.0 °C, aligning with the IPCC AR6 report's best estimate of equilibrium climate sensitivity, which ranges from 2.5 °C to 4 °C.

Our experimental design requires first calculating the emissions from AC use under global warming scenarios, followed by assessing the additional warming effects of these emissions within the given scenario. Exogenous constraints imposed to simulate climate change lead to an internal balancing in the IAM model that any increase in AC emissions, driven by projected CDDs, is offset by emission reductions in other sectors within GCAM, maintaining the integrity of the overall SSP-RCP emission pathway. In this case, we use MAGICC to calculate two temperature outcomes: first, the reference warming result corresponding to the standard SSP-RCP emission pathway; and second, the warming result from the same pathway with the addition of AC-related emissions as calculated by GCAM. The time step for GHG emissions obtained from the GCAM is five years, which does not match one-year time step in MAGICC, so we use a sliding average method to interpolate the emissions for the intermediate years before inputting these values into the MAGICC model. By comparing these two temperature outcomes, we can isolate the additional warming contribution from AC-related emissions. Given that GCAM calculates the range of air conditioning emissions for each SSP-RCP scenario, we utilize the maximum, mean, and minimum values of AC emissions within each scenario to repeat the above MAGICC calculation steps, obtaining a range of potential warming effects from AC use.

Limitations

Owing to limitations in modeling approaches and scenario design, uncertainties persist in our estimates of total warming impact and global inequalities in AC use. Firstly, our analysis adopted a fixed base temperature for CDD calculations across regions. While this approach allows for consistent comparisons across regions and scenarios, it does not account for the potential evolution of comfort thresholds over time. As global temperatures rise, behavioral and physiological adaptations may lead individuals to tolerate higher indoor temperatures before resorting to air conditioning, effectively increasing the base temperature that triggers cooling demand. To provide additional insight and characterize the uncertainty associated with this assumption, we performed a sensitivity analysis using different base temperatures, illustrating how variations in this parameter significantly affect CDD calculations. Secondly, there is a mismatch between the projected AC energy consumption from GCAM and the projected AC stock from our econometric model. GCAM accounts for technological advancements, energy efficiency improvements, and policy influences across regions over time, whereas our econometric model mainly focuses on socioeconomic factors and temperature. Consequently, our analysis's projections of the AC stock do not fully capture the effects of future technological progress or regional disparities. Despite

the mismatch, our findings indicate that the discrepancy between the model-predicted AC stock and the historical data during 2010–2014 is approximately -4.4%, with a range of -2.1% to -5.3%. Both models show consistent trends in the growth of AC stock and energy consumption driven by rising income, temperature, and population, which supports the validity of our overall findings. Lastly, our assessment does not incorporate high-resolution cooling loads analysis, such as monthly, daily or hourly series, which are crucial for understanding peak energy demand and infrastructure stress during periods of extreme temperatures. Regions with considerable seasonal variability, such as South Asia, may experience surges in cooling demand during specific months, placing substantial stress on energy infrastructure and necessitating effective peak load management strategies. Such improvements would provide deeper insights into the dynamics of cooling demand, inform more effective energy infrastructure planning and interventions aimed at mitigating climate impacts while addressing the diverse cooling needs across regions.

Reporting summary

Further information on research design is available in the Nature Portfolio Reporting Summary linked to this article.

Data availability

As mentioned above, this study uses various climate and socioeconomic variables from SSP database²⁹, World bank (<https://www.worldbank.org/en/home>), SEDAC database⁷⁹, Coupled Model Inter-comparison Project Phase 6 (CMIP6)²⁶ and NASA NEX-GDDP-CMIP6 database. First, we use SEDAC database to collect historical and future gridded data of population distribution. Second, we collect climate variables under SSP126, SSP245, SSP370 and SSP585 scenarios with a resolution of 0.25° x 0.25° (25 km in both latitude and longitude resolution) from NASA NEX-GDDP-CMIP6 database, while those under SSP119 from CMIP6 database. The NASA database contains daily average temperature and relative humidity data for the SSP126, SSP245, SSP370, and SSP585 scenarios, but lacks data for the SSP119 scenario. Therefore, we applied the widely used quantile mapping method^{80,81} to calibrate the SSP119 data, and the robustness analysis is shown in Supplementary Table 13. Finally, we construct a sample dataset of 32 regions for 25 years (1990–2014) using historical global AC stock, CDDs, per capita GDP, urbanization rate, which come from IEA⁴ report, CMIP6, NASA and World Bank database. Future per capita GDP and urbanization rate are adopted from SSP database. Source data are provided with this paper for the five main-text figures. Selected regional output data (e.g., electricity consumption structure, power generation structure, CO₂ emissions and non-CO₂ emissions by sector) under different scenarios is also available in Supplementary Data File 1–4. Source data are provided with this paper.

Code availability

The Global Change Analysis Model (GCAM) version 5.2 is an open-source model available at (<https://github.com/JGCRI/gcam-core/releases>). The MAGICC model and its source code is available at (<https://magicc.org>). The additional input files of GCAM and the output of MAGICC are available at (<https://doi.org/10.5281/zenodo.17899891>).

References

1. Forster, P. M. et al. Indicators of Global Climate Change 2022: annual update of large-scale indicators of the state of the climate system and human influence. *Earth Syst. Sci. Data* **15**, 2295–2327 (2023).
2. Zhao, Q. et al. Global, regional, and national burden of mortality associated with non-optimal ambient temperatures from 2000 to 2019: a three-stage modelling study. *Lancet Planet Health* **5**, e415–e425 (2021).

3. Peng, R. D. et al. Toward a quantitative estimate of future heat wave mortality under global climate change. *Environ. Health Perspect.* **119**, 701–706 (2011).
4. IEA. *The Future of Cooling*. <https://www.iea.org/reports/the-future-of-cooling> (2018).
5. Davis, L. W. & Gertler, P. J. Contribution of air conditioning adoption to future energy use under global warming. *Proc. Natl. Acad. Sci. USA* **112**, 5962–5967 (2015).
6. JRAIA. World Air Conditioner Demand by Region. (The Japan Refrigeration and Air Conditioning Industry Association, Tokyo, 2010–2022).
7. Zhou, Y. et al. Modeling the effect of climate change on U.S. state-level buildings energy demands in an integrated assessment framework. *Appl. Energy* <https://doi.org/10.1016/j.apenergy.2013.08.034> (2014).
8. Waite, M. et al. Global trends in urban electricity demands for cooling and heating. *Energy* **127**, 786–802 (2017).
9. Pavanello, F. et al. Air-conditioning and the adaptation cooling deficit in emerging economies. *Nat. Commun.* **12**, 6460 (2021).
10. Wang, Z. et al. Trade-Offs between Direct Emission Reduction and Intersectoral Additional Emissions: Evidence from the Electrification Transition in China's Transport Sector. *Environ. Sci. Tech.* <https://doi.org/10.1021/acs.est.3c00556> (2023).
11. IPCC. Climate Change 2007: Synthesis Report. Contribution of Working Groups I, II and III to the Fourth Assessment Report of the Intergovernmental Panel on Climate Change [Core Writing Team, Pachauri, R.K. and Reisinger, A. (eds.)]. (IPCC, Geneva, Switzerland, 2007).
12. Sharifi, A. & Yamagata, Y. Principles and criteria for assessing urban energy resilience: A literature review. *Renew. Sustain. Energy Rev.* **60**, 1654–1677 (2016).
13. Morecroft, M. D. et al. Measuring the success of climate change adaptation and mitigation in terrestrial ecosystems. *Science* <https://doi.org/10.1126/science.aaw9256> (2019).
14. Mazzone, A. et al. Understanding systemic cooling poverty. *Nat. Sustain.* <https://doi.org/10.1038/s41893-023-01221-6> (2023).
15. Li, D., Yuan, J. & Kopp, R. E. Escalating global exposure to compound heat-humidity extremes with warming. *Environ. Res. Lett.* <https://doi.org/10.1088/1748-9326/ab7d04> (2020).
16. Spinoni, J. et al. Changes of heating and cooling degree-days in Europe from 1981 to 2100. *Int. J. Climatol.* **38**, e191–e208 (2018).
17. Clarke, L. et al. Effects of long-term climate change on global building energy expenditures. *Energy Econ.* **72**, 667–677 (2018).
18. Cheng, J. et al. A synergistic approach to air pollution control and carbon neutrality in China can avoid millions of premature deaths annually by 2060. *One Earth* **6**, 978–989 (2023).
19. Calvin, K. et al. The SSP4: a world of deepening inequality. *Glob. Environ. Change* **42**, 284–296 (2017).
20. Wigley, T. M. L. et al. Uncertainties in climate stabilization. *Climatic Change* **97**, 85–121 (2009).
21. Meinshausen, M. et al. The shared socio-economic pathway (SSP) greenhouse gas concentrations and their extensions to 2500. *Geosci. Model Dev.* **13**, 3571–3605 (2020).
22. Nicholls, Z. et al. Changes in IPCC Scenario Assessment Emulators Between SR1.5 and AR6 Unraveled. *Geophys Res Lett.* **49**, e2022GL099788 (2022).
23. IPCC. Climate Change 2021: The Physical Science Basis. Contribution of Working Group I to the Sixth Assessment Report of the Intergovernmental Panel on Climate Change. 2391 (Cambridge, United Kingdom and New York, NY, USA, 2021).
24. IPCC, 2022: *Climate Change: Impacts, Adaptation and Vulnerability*. Contribution of Working Group II to the Sixth Assessment Report of the Intergovernmental Panel on Climate Change. Cambridge University Press. (Cambridge, UK and New York, NY, USA 2022), 3056, <https://doi.org/10.1017/9781009325844>.
25. Thrasher, B. et al. NASA Global Daily Downscaled Projections, CMIP6. *Sci. Data* **9**, 262 (2022).
26. Eyring, V. et al. Overview of the coupled model intercomparison project phase 6 (CMIP6) experimental design and organization. *Geosci. Model Dev.* **9**, 1937–1958 (2016).
27. O'Neill, B. C. et al. A new scenario framework for climate change research: the concept of shared socioeconomic pathways. *Climatic Change* **122**, 387–400 (2014).
28. Kriegler, E. et al. A new scenario framework for climate change research: the concept of shared climate policy assumptions. *Climatic Change* **122**, 401–414 (2014).
29. Riahi, K. et al. The Shared Socioeconomic Pathways and their energy, land use, and greenhouse gas emissions implications: An overview. *Glob. Environ. Change* **42**, 153–168 (2017).
30. van Vuuren, D. P. et al. The representative concentration pathways: an overview. *Climatic Change* **109**, 5–31 (2011).
31. Gao, J. Global 1-km Downscaled Population Base Year and Projection Grids Based on the Shared Socioeconomic Pathways, Revision 01. <https://doi.org/10.7927/q7z9-9r69> (2020).
32. Gao, J. Downscaling Global Spatial Population Projections from 1/8-degree to 1-km Grid Cells. (2017).
33. Andreae, M. O., Jones, C. D. & Cox, P. M. Strong present-day aerosol cooling implies a hot future. *Nature* **435**, 1187–1190 (2005).
34. Dvorak, M. T. et al. Estimating the timing of geophysical commitment to 1.5 and 2.0 °C of global warming. *Nat. Clim. Change* **12**, 547–552 (2022).
35. Undorf, S. et al. Detectable Impact of Local and Remote Anthropogenic Aerosols on the 20th Century Changes of West African and South Asian Monsoon Precipitation. *J. Geophys. Res.: Atmospheres* **123**, 4871–4889 (2018).
36. Biardeau, L. T., Davis, L. W., Gertler, P. & Wolfram, C. Heat exposure and global air conditioning. *Nat. Sustainability* **3**, 25–28 (2019).
37. Andrijevic, M., Byers, E., Mastrucci, A., Smits, J. & Fuss, S. Future cooling gap in shared socioeconomic pathways. *Environmental Research Letters* **16**, <https://doi.org/10.1088/1748-9326/ac2195> (2021).
38. Davis, L., Gertler, P., Jarvis, S. & Wolfram, C. Air conditioning and global inequality. *Global Environmental Change* **69**, <https://doi.org/10.1016/j.gloenvcha.2021.102299> (2021).
39. Sneha Sachar, Iain Campbell & Kalanki, A. Solving the global cooling challenge: How to counter the climate threat from room air conditioners. (2018).
40. Isaac, M. & van Vuuren, D. P. Modeling global residential sector energy demand for heating and air conditioning in the context of climate change. *Energy Policy* **37**, 507–521 (2009).
41. Mastrucci, A., van Ruijven, B., Byers, E., Poblete-Cazenave, M. & Pachauri, S. Global scenarios of residential heating and cooling energy demand and CO2 emissions. *Clim. Change* <https://doi.org/10.1007/s10584-021-03229-3> (2021).
42. Colelli, F. P., Wing, I. S. & Cian, E. Air-conditioning adoption and electricity demand highlight climate change mitigation-adaptation tradeoffs. *Sci. Rep.* **13**, 4413 (2023).
43. Climate Watch data: Climate Watch. 2022. GHG Emissions. Washington, DC: World Resources Institute. <https://www.climatewatchdata.org/ghg-emissions>.
44. Kibria M T, et al. Assessment of environmental impact for air-conditioning systems in Japan using HFC based refrigerants. *Evergreen*, **6**, 246–253. <https://doi.org/10.5109/2349301> (2019).
45. IPCC. *Climate Change 2014: Synthesis Report. Contribution of Working Groups I, II and III to the Fifth Assessment Report of the Intergovernmental Panel on Climate Change*. IPCC, Geneva, Switzerland, 151 (2014).
46. Tokarska, K. B. et al. Past warming trend constrains future warming in CMIP6 models. *Sci. Adv.* **6**, eaaz9549 (2020).

47. Coronese, M., Lamperti, F., Keller, K., Chiaromonte, F. & Roventini, A. Evidence for sharp increase in the economic damages of extreme natural disasters. *Proc. Natl. Acad. Sci. USA* **116**, 21450–21455 (2019).
48. Hsiang, S. M. Temperatures and cyclones strongly associated with economic production in the Caribbean and Central America. *Proc. Natl. Acad. Sci. USA* **107**, 15367–15372 (2010).
49. Zhao, H. et al. Inequality of household consumption and air pollution-related deaths in China. *Nat. Commun.* **10**, 4337 (2019).
50. IPCC. Climate Change 2023: Synthesis Report. Contribution of Working Groups I, II and III to the Sixth Assessment Report of the Intergovernmental Panel on Climate Change. 35–115 (IPCC, Geneva, Switzerland, 2023).
51. Kondo, K., Mabon, L., Bi, Y., Chen, Y. & Hayabuchi, Y. Balancing conflicting mitigation and adaptation behaviours of urban residents under climate change and the urban heat island effect. *Sustain. Cities Soc.* **65**, 102585 (2021).
52. Tremeac, B. et al. Influence of air conditioning management on heat island in Paris air street temperatures. *Appl. Energy* **95**, 102–110 (2012).
53. Sarofim, M. C. & Reilly, J. M. Applications of integrated assessment modeling to climate change. *WIREs Clim. Change* **2**, 27–44 (2010).
54. Boudali Errebai, F., Strebel, D., Carmeliet, J. & Derome, D. Impact of urban heat island on cooling energy demand for residential building in Montreal using meteorological simulations and weather station observations. *Energy Build.* <https://doi.org/10.1016/j.enbuild.2022.112410> (2022).
55. Santamouris, M. Analyzing the heat island magnitude and characteristics in one hundred Asian and Australian cities and regions. *Sci. Total Environ.* **512–513**, 582–598 (2015).
56. Malik, A. et al. The potential for indoor fans to change air conditioning use while maintaining human thermal comfort during hot weather: an analysis of energy demand and associated greenhouse gas emissions. *Lancet Planet Health* **6**, e301–e309 (2022).
57. Dong, Y., Coleman, M. & Miller, S. A. Greenhouse gas emissions from air conditioning and refrigeration service expansion in developing countries. *Annu. Rev. Environ. Resour.* **46**, 59–83 (2021).
58. Huang, H. et al. Optimum insulation thicknesses and energy conservation of building thermal insulation materials in Chinese zone of humid subtropical climate. *Sustainable Cities and Society* **52**, <https://doi.org/10.1016/j.scs.2019.101840> (2020).
59. Somasundaram, S., Chong, A., Wei, Z. & Thangavelu, S. R. Energy saving potential of low-e coating based retrofit double glazing for tropical climate. *Energy Build.* <https://doi.org/10.1016/j.enbuild.2019.109570> (2020).
60. Elsaid, A. M. A novel design, implementation and performance evaluation of the first electronic expansion ejector for energy saving of a mini split air conditioner controlled by inverter. *Energy Convers. Manag.* <https://doi.org/10.1016/j.enconman.2022.115603> (2022).
61. Wilson, E. J. H., Munankarmi, P., Less, B. D., Reyna, J. L. & Rothgeb, S. Heat pumps for all? distributions of the costs and benefits of residential air-source heat pumps in the United States. *Joule* **8**, 1000–1035 (2024).
62. He, Z., Hong, T. & Chou, S. K. A framework for estimating the energy-saving potential of occupant behaviour improvement. *Appl. Energy* <https://doi.org/10.1016/j.apenergy.2021.116591> (2021).
63. Darwazeh, D., Duquette, J., Gunay, B., Wilton, I. & Shillinglaw, S. Review of peak load management strategies in commercial buildings. *Sustain. Cities and Soc.* <https://doi.org/10.1016/j.scs.2021.103493> (2022).
64. Li, X., Chen, S., Li, H., Lou, Y. & Li, J. Multi-dimensional analysis of air-conditioning energy use for energy-saving management in university teaching buildings. *Build. Environ.* <https://doi.org/10.1016/j.buildenv.2020.107246> (2020).
65. Wang, Y., Xu, Z., Wang, Z. & Li, H. Analysis of thermal energy saving potentials through adjusting user behavior in hotel buildings of the Yangtze River region. *Sustain. Cities Soc.* <https://doi.org/10.1016/j.scs.2019.101724> (2019).
66. Calvin, K. et al. GCAM v5.1: representing the linkages between energy, water, land, climate, and economic systems. *Geosci. Model Dev.* **12**, 677–698 (2019).
67. van Vuuren, D. P. et al. A new scenario framework for Climate Change Research: scenario matrix architecture. *Climatic Change* **122**, 373–386 (2013).
68. Maia-Silva, D., Kumar, R. & Nateghi, R. The goldilocks zone in cooling demand: what can we do better? *Earth's Future* **10**, e2021EF002476 (2022).
69. Lu, Y.-C. & Roms, D. M. Extending the Heat Index. *J. Appl. Meteorol. Climatol.* **61**, 1367–1383 (2022).
70. Woods, J. et al. Humidity's impact on greenhouse gas emissions from air conditioning. *Joule* **6**, 726–741 (2022).
71. Hartin, C. et al. Integrated modeling of human-earth system interactions: An application of GCAM-fusion. *Energy Econ.* **103**, 105566 (2021).
72. Miranda, N. D. et al. Change in cooling degree days with global mean temperature rise increasing from 1.5 °C to 2.0 °C. *Nature Sustainability*, <https://doi.org/10.1038/s41893-023-01155-z> (2023).
73. Levesque, A. et al. How much energy will buildings consume in 2100? a global perspective within a scenario framework. *Energy* **148**, 514–527 (2018).
74. Dekker, M. M. et al. Identifying energy model fingerprints in mitigation scenarios. *Nat. Energy* **8**, 1395–1404 (2023).
75. Park, C. et al. Avoided economic impacts of energy demand changes by 1.5 and 2 °C climate stabilization. *Environ. Res. Lett.* <https://doi.org/10.1088/1748-9326/aab724> (2018).
76. Diffenbaugh, N. S. & Burke, M. Global warming has increased global economic inequality. *Proc. Natl. Acad. Sci. USA* **116**, 9808–9813 (2019).
77. Kikstra, J. S. et al. The IPCC sixth assessment report WGIII climate assessment of mitigation pathways: from emissions to global temperatures. *Geosci. Model Dev.* **15**, 9075–9109 (2022).
78. Meinshausen, M., Raper, S. C. B. & Wigley, T. M. L. Emulating coupled atmosphere-ocean and carbon cycle models with a simpler model, MAGICC6 – Part 1: Model description and calibration. *Atmos. Chem. Phys.* **11**, 1417–1456 (2011).
79. SEDAC. Gridded Population of the World, Version 4.11 (GPWv4): Population Count, Revision 11. NASA Socioeconomic Data and Applications Center (SEDAC) (2018).
80. Grillakis, M. G., Koutroulis, A. G., Daliakopoulos, I. N. & Tsanis, I. K. A method to preserve trends in quantile mapping bias correction of climate modeled temperature. *Earth Syst. Dyn.* **8**, 889–900 (2017).
81. de Souza Ferreira, G. W. et al. Assessment of the wind power density over South America simulated by CMIP6 models in the present and future climate. *Clim. Dyn.* **62**, 1729–1763 (2023).
82. Fantom, N. J. & Serajuddin, U. *The World Bank's classification of countries by income*. World bank policy research working paper 7528 (2016).
83. van Ruijven, B. J., De Cian, E. & Sue Wing, I. Amplification of future energy demand growth due to climate change. *Nat. Commun.* **10**, 2762 (2019).

Acknowledgements

This work is supported by the National Natural Science Foundation of China (Reference No. 72321002, 72504028, 72243001, 72074026, 72141302, 72222017, 72311530105 and 72361137002), Youth Project of Humanities and Social Sciences Program of Ministry of Education (Grant No. 25YJC790077), Key Projects of Philosophy and Social Sciences Program of Ministry of Education (Reference No. 21JZD027), Major project of National Social Science Foundation (Reference No. 22&ZD104),

The Royal Society International Exchanges (IEC\NSFC\223059), Humanities and Social Sciences Cultivation Program, Kunming University of Science and Technology, China (Grant No. SKPYYB202508), the European Union's Horizon Europe research and innovation programme (PANTHEON , Grant No.101137905).

Author contributions

H.Z., Y.S., Z.S. and Z.W. designed the research. H.Z. and Y.S. led the study and drafted the manuscript. H.Z., Y.S. and F.Y. completed MAGICC and GCAM modeling work. R.X., J.M., B.W., S.F., H.Z. and Y.S. completed the panel OLS model. Z.W., K.H., R.L., J.K., B.Z. and Z.S. contributed efforts to the revision and editing of the manuscript.

Competing interests

The authors declare no competing interests.

Additional information

Supplementary information The online version contains supplementary material available at <https://doi.org/10.1038/s41467-026-69393-1>.

Correspondence and requests for materials should be addressed to Yuli Shan or Zhaohua Wang.

Peer review information *Nature Communications* thanks Hongxun Liu, Jorge Moreno and Ida Sognnaes for their contribution to the peer review of this work. A peer review file is available.

Reprints and permissions information is available at <http://www.nature.com/reprints>

Publisher's note Springer Nature remains neutral with regard to jurisdictional claims in published maps and institutional affiliations.

Open Access This article is licensed under a Creative Commons Attribution-NonCommercial-NoDerivatives 4.0 International License, which permits any non-commercial use, sharing, distribution and reproduction in any medium or format, as long as you give appropriate credit to the original author(s) and the source, provide a link to the Creative Commons licence, and indicate if you modified the licensed material. You do not have permission under this licence to share adapted material derived from this article or parts of it. The images or other third party material in this article are included in the article's Creative Commons licence, unless indicated otherwise in a credit line to the material. If material is not included in the article's Creative Commons licence and your intended use is not permitted by statutory regulation or exceeds the permitted use, you will need to obtain permission directly from the copyright holder. To view a copy of this licence, visit <http://creativecommons.org/licenses/by-nc-nd/4.0/>.

© The Author(s) 2026